Neuroradiology (2021) 63:373–380
https://doi.org/10.1007/s00234-021-02635-9

SPINAL NEURORADIOLOGY

Spatial correspondence of spinal cord white matter tracts using diffusion tensor imaging, fibre tractography, and atlas-based segmentation

Stewart McLachlin[1] · Jason Leung[2] · Vignesh Sivan[2] · Pierre-Olivier Quirion[3] · Phoenix Wilkie[2] · Julien Cohen-Adad[3] · Cari Marisa Whyne[2,4] · Michael Raymond Hardisty[2,4]

Received: 17 September 2020 / Accepted: 5 January 2021 / Published online: 14 January 2021

Abstract

Purpose Neuroimaging provides great utility in complex spinal surgeries, particularly when anatomical geometry is distorted by pathology (tumour, degeneration, etc.). Spinal cord MRI diffusion tractography can be used to generate streamlines; however, it is unclear how well they correspond with white matter tract locations along the cord microstructure. The goal of this work was to evaluate the spatial correspondence of DTI tractography with anatomical MRI in healthy anatomy (where anatomical locations can be well defined in T1-weighted images).

Methods Ten healthy volunteers were scanned on a 3T system. T1-weighted (1 × 1 × 1 mm) and diffusion-weighted images (EPI readout, 2 × 2 × 2 mm, 30 gradient directions) were acquired and subsequently registered (Spinal Cord Toolbox (SCT)). Atlas-based (SCT) anatomic label maps of the left and right lateral corticospinal tracts were identified for each vertebral region (C2–C6) from T1 images. Tractography streamlines were generated with a customized approach, enabling seeding of specific spinal tract regions corresponding to individual vertebral levels. Spatial correspondence of generated fibre streamlines with anatomic tract segmentations was compared in unseeded regions of interest (ROIs).

Results Spatial correspondence of the lateral corticospinal tract streamlines was good over a single vertebral ROI (Dice's similarity coefficient (DSC) = 0.75 ± 0.08, Hausdorff distance = 1.08 ± 0.17 mm). Over larger ROI, fair agreement between tractography and anatomical labels was achieved (two levels: DSC = 0.67 ± 0.13, three levels: DSC = 0.52 ± 0.19).

Conclusion DTI tractography produced good spatial correspondence with anatomic white matter tracts, superior to the agreement between multiple manual tract segmentations (DSC ~ 0.5). This supports further development of spinal cord tractography for computer-assisted neurosurgery.

Keywords Spinal cord · Diffusion tensor imaging · Tractography · Segmentation · Deformable registration

Introduction

Diffusion tensor imaging (DTI) enables characterization of the location and integrity of white matter (WM) tracts in neural tissues [1]. Connectivity of the neural tissue can be obtained using fibre tractography methods to generate three-dimensional (3D) streamlines based on analysis of water diffusion anisotropy [2]. DTI tractography has shown great utility in identifying and quantifying neural structures even in the presence of geometric distortions secondary to pathology [3, 4].

The use of DTI tractography is rapidly becoming the standard of care for neurosurgical procedures in the brain. DTI tractography has been particularly useful in indications that involve geometric uncertainty and distortion (i.e. tumour, congenital defects) with applications in clinical decision-making,

✉ Michael Raymond Hardisty
michael.hardisty@sunnybrook.ca

[1] Department of Mechanical and Mechatronics Engineering, University of Waterloo, 200 University Avenue West, E7 3424, Waterloo, Ontario N2L 3G1, Canada

[2] Orthopaedic Biomechanics Laboratory, Sunnybrook Research Institute, 2075 Bayview Ave, S621, Toronto, Ontario M4N 3M5, Canada

[3] Department of Electrical Engineering, Polytechnique Montreal, Ecole Polytechnique, Pavillon Lassonde, 2700 Ch de la Tour, L-5610, Montréal, Quebec H3T 1N8, Canada

[4] Department of Surgery, University of Toronto, 2075 Bayview Ave, S621, Toronto, Ontario M4N 3M5, Canada

disease characterization, surgical planning, and navigation. This approach has enabled the identification and precise localization of very small WM tracts when registered to anatomical T1- or T2-weighted MRI scans, allowed for the analysis of tract-specific health, and has been used for image-guided brain tumour resections [5]. The development and implementation of clinically viable image acquisition and automated processing techniques has improved the clinical adoption of these new technologies [6, 7].

DTI tractography streamlines show connection and directionality of axonal tissue, allowing the depiction of white matter fibres. In the brain, the direction of these white matter tracts can be used to identify anatomical pathways that are related to specific functional domains and aid in the classification of neural tissue. However, in the spinal cord, the fibre direction of the white matter does not encode information about function, as fibres primarily go in the superior-inferior direction. Nevertheless, DTI of the spinal cord has recently started to gain attention as a possible tool to improve clinical decision-making [3, 7–12]. A growing number of researchers and clinicians are innovating new MRI acquisition and analysis techniques to overcome the challenges of spinal cord DTI [13]. Spinal cord tractography generated via DTI can be used to generate streamlines [3, 8, 14, 15]; however, it is unclear how well they spatially correspond with anatomic white matter tract locations along the cord microstructure. Good correspondence of streamlines with anatomical structures and an understanding of limitations is crucial for guiding interventions. Spinal cord-specific challenges arise due to physiologic motion (particularly in the cervical spinal cord), its small cross-section, and the susceptibility of the surrounding vertebral bone to introduce image artefacts [11, 16].

The Spinal Cord Toolbox (SCT) software package has been developed to assist with the analysis of spinal cord imaging, including state-of-the-art tools for identifying spinal cord anatomy, deformable image registration, segmentation, and quantification [17]. SCT has established methods for atlas-based segmentation and labelling of white matter tracts of the spinal cord [18–21]. Most tools in SCT are focused on quantitative metrics, with no current implementation of fibre tractography techniques. Spinal cord tractography using tract-specific streamlines (Fig. 1) may be useful for assessing white matter connectivity specifically in clinical scenarios where anatomical and geometric imaging distortions present at focal sites, such as in the presentation of spinal cord tumours [3, 8, 15]. An opportunity exists to extend computer-assisted neurosurgical applications of DTI tractography into the spine through the SCT platform, specifically to create tools to aid in the planning and execution of complex spinal surgeries. This technology could assist in surgeries where there is anatomical uncertainty, potentially allowing for 3D visualization of specific white matter tracts.

The purpose of this study was to investigate the concept of using DTI tractography to determine the location of individual spinal cord white matter tracts. Specifically, this study evaluated the spatial correspondence of DTI tractography against white matter tracts identified with anatomical T1-weighted images of healthy spinal cord anatomy. It was hypothesized that DTI tractography streamlines could achieve accurate spatial correspondence to atlas-based segmentations of anatomical white matter tracts identified with T1-weighted imaging.

Materials and methods

Image acquisition

Ten healthy volunteer subjects (mean age 32 ± 7 years old, 7 men and 3 women) were scanned using a 3T MRI system (Trio Tim, Siemens Healthcare, Erlangen, Germany) with a 4-channel neck Rx coil in accordance with a research protocol, including informed consent, approved by the Institutional Review Board of York University. Image acquisition sequences consisted of (1) a T1-weighted MPRAGE (TR = 2300 ms, TE = 3.41 ms, flip angle = 9°, FOV = 256 × 256 mm^2, 160 slices, 1 × 1 × 1 mm^3, standard shim mode) covering the C1–C7 cervical vertebrae and (2) a single-shot EPI sequence of diffusion-weighted images with 30 gradient directions (at a b value of 800 s/mm^2) and two b = 0 images,

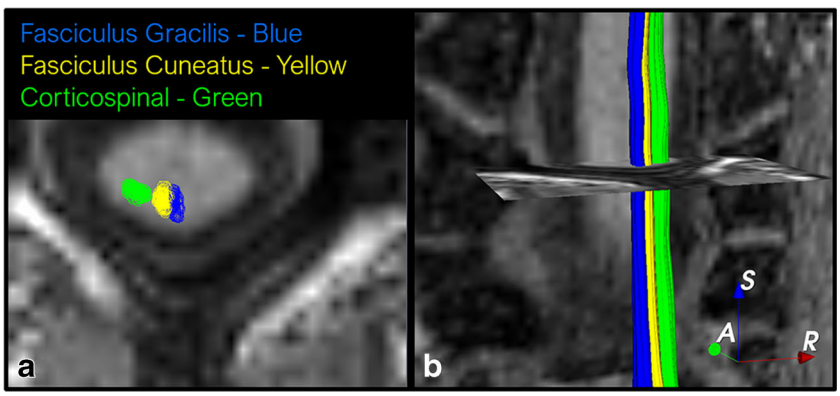

Fig. 1 Example of spinal cord tractography using labelled white matter streamlines of the dorsal columns, shown in **a** 2D axial view and **b** 3D isometric view. Tract-specific streamlines may help examine white matter connectivity in clinical scenarios involving track disruptions and distortions

covering the C2–C6 vertebrae (image matrix = 256 × 256 mm^2, voxel size 2 × 2 × 2 mm^3, not cardiac gated). The image acquisition protocol was decided upon to balance imaging time and image resolution required for the template-based registration process described below. To correct for susceptibility artefacts, diffusion-weighted images were collected in the transverse direction with reversed anteroposterior phase-encode blips to create image pairs with distortions of opposite direction. From these pairs, the susceptibility-induced off-resonance field was estimated (see the 'Image processing' section). The total scan time of the T1 and DTI image sequences was approximately 10 min.

Image processing

An automated spinal cord DTI processing pipeline was developed to generate tractography-derived tract-specific streamlines from diffusion and T1 MRI. A custom image processing pipeline was established for this study using open-source tools in both SCT and 3D Slicer software [22, 23]. Motion- and susceptibility-induced artefacts were corrected using a method similar to that described by Andersson et al., as implemented in FSL [24, 25]. The automated image processing steps in the pipeline included tensor fitting, spinal cord segmentation, T1-DWI deformable image registration, tensor field warping, and tractography streamline calculations (Fig. 2) [26, 27].

Spinal cord geometry was segmented and labelled with the cervical vertebral level (PropSeg and Label Vertebrae tools, SCT v2.2) [21]. Segmentation by deformable registration of SCT atlas volumes of the spinal cord white matter tracts defined tract geometry (Fig. 3) [19]. Anatomic label maps (i.e. segmentations) of individual tract geometries for each of the cervical vertebrae were subsequently generated from the SCT atlas (threshold = 50%) for two larger white matter tracts: the left and right lateral corticospinal tracts (Fig. 3). This investigation focused on the assessment of these specific tracts due to the recognized importance of identifying these structures in posterior surgical approaches as disruption of these tracts leads to known deficits in motor control and decreased patient quality of life [28].

Registration and segmentation of the diffusion space was performed with methods within SCT. The spinal cord was defined in the diffusion space by propagating a deformable model (PropSeg tool) to segment the mean of the diffusion gradient volumes. The atlas within SCT was deformably registered to the mean of the diffusion gradient volumes, establishing tract regions in the diffusion space and the mapping between the anatomical and diffusion space via the atlas space (diffusion ↔ atlas ↔ anatomical). After determination of the spatial mapping from the diffusion space to the anatomical, transformation of the tensor information was done using a technique based on preservation of the principal direction [26]. In brief, this approach computes the Jacobian at each voxel location from the deformation field and uses the Jacobian to transform the tensors. Tensors were transformed by rotating the first eigenvector of the tensor and renormalizing, then a rotation matrix is determined such that the second eigenvector remains normal to the first. Image registration methods were confirmed by manual inspection and evaluation of tractography and anatomical label agreement below.

DTI tractography

Tensors were estimated using a weighted least squares algorithm (3D Slicer, Teem Library, https://github.com/Slicer/teem). A deterministic tractography algorithm based on hyper-streamlines (3D Slicer, SlicerDMRI, https://github.com/SlicerDMRI) was used to generate tractography streamlines by seeding defined label map volumes using a fractional anisotropy threshold (seed spacing = 0.5 mm, start/stop threshold = 0.3/0.15, stopping curvature = 45°, minimum streamline length = 20 mm) [23, 29]. Rather than seeding the entire diffusion image volume, the SCT-based pipeline developed for this work allowed for selection of specific spinal tract label maps, representing tracts at specific vertebral levels in the cervical spine, for seeding the tractography algorithm, resulting in streamlines labelled by spinal tract (Fig. 1).

Data analysis

The processing pipeline was evaluated in this study by examining the spatial correspondence of label maps

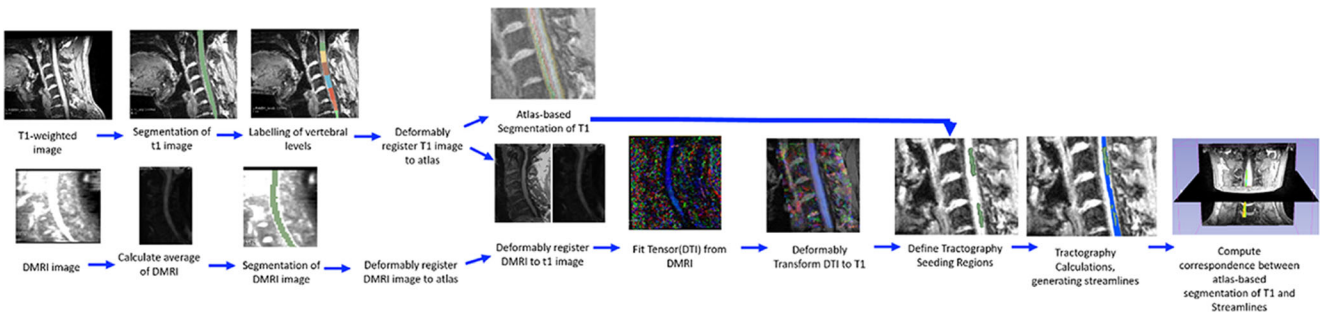

Fig. 2 Flow chart of automated tractography pipeline steps. Inputs: T1-weighted images and DMRI volumes. Outputs: Streamlines labelled by anatomical tract, segmentation of T1, and characterization agreement between anatomically derived labels and streamlines

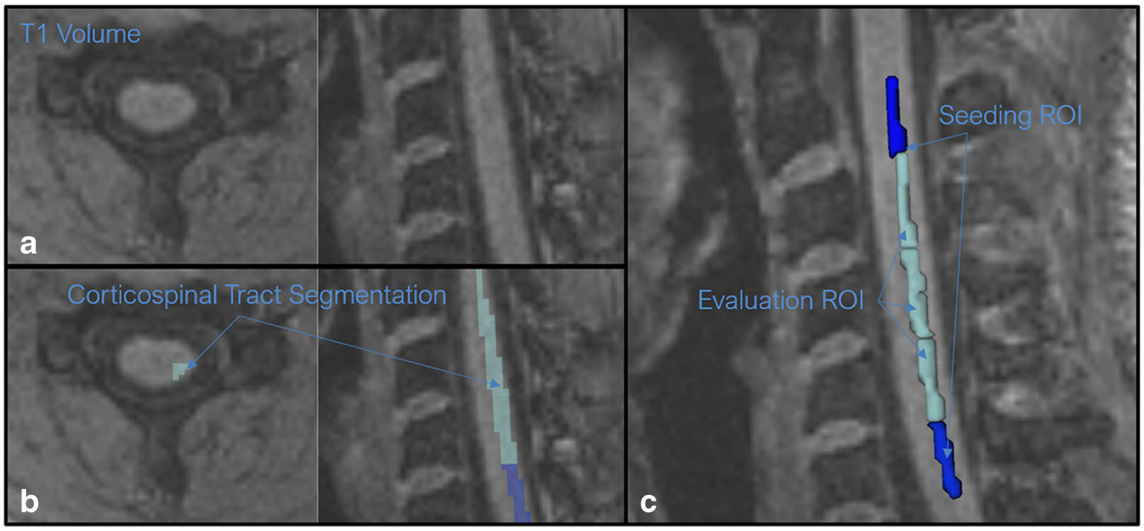

Fig. 3 **a** Axial and sagittal views of the original T1 image. **b** Anatomic label maps of the corticospinal tract (generated using a probabilistic atlas volume generated with Spinal Cord Toolbox, 50% threshold). **c** Regions of interest (ROIs) were used for seeding and evaluation of streamline spatial correspondence. In this example, two levels are used for seeding tractography (C2 and C6, shown in dark blue) and three unseeded levels (C3–C5, light blue) are used for evaluation of the spatial correspondence of the streamline versus the anatomic label maps

generated via DTI-derived streamlines, transformed to the anatomical space, with the anatomic label maps from the SCT atlas. Tractography streamlines were compared against atlas-based anatomical labels in a region of interest (ROI), defined as spinal cord regions ranging from one to three vertebral levels. The tractography streamlines were not seeded in these regions (Fig. 3c); only streamlines which followed into these ROIs from the seeded cord regions in the adjacent cranial and caudal vertebral levels were compared to the anatomical white matter segmentations. This was necessary to avoid biased results and to simulate possible clinical scenarios where geometric distortions due to pathology may exist at focal vertebral levels and preclude seeding in these regions. For the datasets in the current study, the seeded cord regions were as follows: C3 and C5 seeded for a single skipped level (C4), C3 and C6 seeded for two skipped levels (C4 and C5), and C2 and C6 seeded for three skipped levels (C3, C4, and C5).

The spatial correspondence of the anatomical tract label maps and diffusion-based streamlines in the ROI were evaluated by calculating Dice's similarity coefficient (DSC, DiceComputation module in 3D Slicer) and the distance between the structures based on the average distance (AD) and the Hausdorff distance (HD). DSC was evaluated by defining a diffusion-derived label field from the tract-specific tractography streamlines. Voxels with streamlines passing through were labelled with the streamline label for the DSC computation. Additionally, the volume of these anatomic and diffusion-based label maps was calculated along with the percentage of streamlines passing within the anatomical tract label.

Results

Streamlines across the evaluated levels were successfully generated for each of the white matter tracts using the described seeding constraints of the label maps. The entire automated pipeline ran in approximately 15 min for each subject's dataset, without any manual intervention. More than 99% of all streamlines generated passed within the corresponding anatomic tract label (Fig. 4). The number of skipped levels however did affect the spatial correspondence between the anatomic tracts and diffusion streamlines (Table 1). Spatial correspondence of the lateral corticospinal streamlines demonstrated good agreement with the left and right anatomical labels across a single skipped vertebral ROI (left tract: DSC = 0.74 ± 0.08, right tract: DSC = 0.77 ± 0.07). For larger ROI, there was fair agreement in the anatomic and streamline correspondence for two (left tract: DSC = 0.65 ± 0.16, right tract: DSC = 0.69 ± 0.09) and three (left tract: DSC = 0.51 ± 0.20, right tract: DSC = 0.52 ± 0.19) skipped vertebral levels (Fig. 5, showing 3 skipped levels). Distances between the streamlines and anatomical labels showed good spatial correspondence and a similar trend with best agreement when considering a single level (HD = 1.08 ± 0.17 mm, AD = 0.14 ± 0.06 mm) with worse performance for two (HD = 1.41 ± 0.39 mm, AD = 0.20 ± 0.10 mm) and three (HD = 1.77 ± 0.41 mm, AD = 0.30 ± 0.13 mm) vertebral levels. Volumetric comparison of the anatomic and diffusion-based label maps again showed a similar trend as DSC and distance with the best agreement for evaluation of a single level (92.83 ± 18.35 mm^3 vs. 98.43 ± 15.86 mm^3) and worse agreement with larger ROI, with the biggest difference at three levels (230.89 ± 55.34 mm^3 vs.

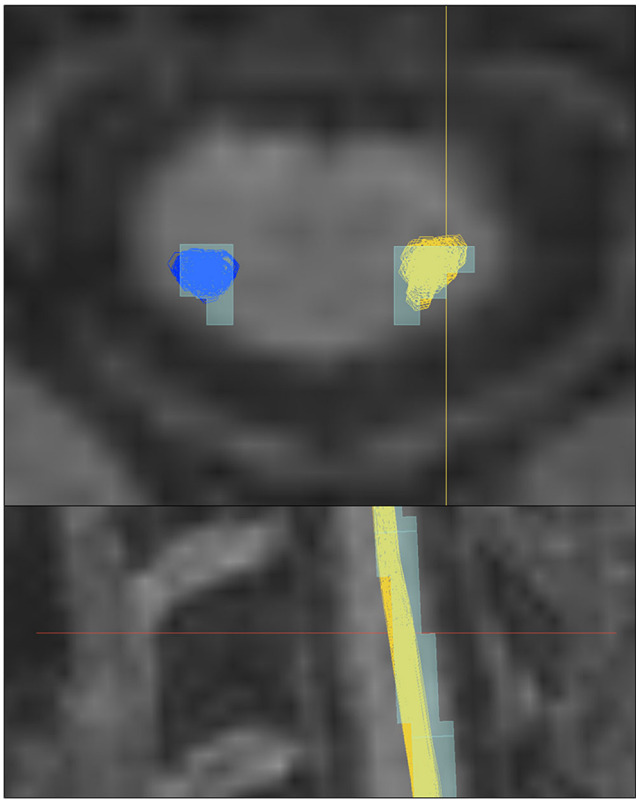

Fig. 4 Qualitative comparison of streamlines (shown as dark blue and yellow tubes) and atlas-based anatomical segmentation (light blue shaded voxels) of the left and right lateral corticospinal tracts overlaid on T1-weighted images of the axial (top) and lateral (bottom) slices in ROI not used to seed tractography. For the dark blue streamlines shown on the axial slice, agreement between the overlapping streamline tubes and voxels would be approximately 80% (4 out of 5 voxels covered)

165.08 ± 84.09 mm^3 for the diffusion and anatomic label map volumes respectively).

Discussion

This study explored the concept of using a white matter atlas from T1-weighted images to seed and evaluate tractography in the spinal cord. Results from this pilot study in healthy control subjects found that the spatial correspondence between streamlines and anatomical labels was good (for a single level ROI) to fair (for multiple skipped levels) for the left and right lateral corticospinal tracts of the spinal cord. This spatial correspondence between DTI and T1 was better than previously reported data for multiple manual segmentations (DSC ~ 0.5) [19]. This is likely due to the automated image processing pipeline that eliminated the need for manual segmentations. Inaccuracies in the larger evaluation regions were in part due to fewer streamlines being generated by the pipeline, as the pipeline selected only streamlines which passed through both the proximal and distal seeding regions.

The implementation of spinal cord visualization using DTI tractography has a number of potential clinical use cases [6, 16, 30–32]. Spinal cord tractography could assist with status evaluation following track disruption resulting from compressive myelopathy or brachial plexus avulsion, or in the case of identifying anatomic tract disruptions from tumours or dysraphism, and finally in follow-up to functional recovery for multiple sclerosis and postoperative surgery. Recently, DTI has been shown as a valuable tool to assess the severity and predict outcome in patients with cervical spinal myelopathy [14, 28, 33]. Additional studies have supported the ability of DTI and corresponding fibre tractography to identify the exact location of intramedullary spinal cord tumours based on displaced WM tracts and predict the respectability of these tumours [3, 8]. These rare, but devastating, intramedullary tumours of the cord have been treated surgically by entering the spinal cord with a

Table 1 Summary of the Dice's similarity coefficient measurements between the anatomical tract label maps and diffusion-based streamlines over the region of interest defined by the number of skipped vertebral levels

	Left lateral corticospinal tract			Right lateral corticospinal tract		
Subject	1 level skipped	2 levels skipped	3 levels skipped	1 level skipped	2 levels skipped	3 levels skipped
1	0.76	0.74	0.65	0.77	0.73	0.48
2	0.67	0.55	0.20	0.78	0.65	0.12
3	0.77	0.87	0.75	0.80	0.78	0.66
4	0.58	0.60	0.56	0.58	0.60	0.56
5	0.84	0.74	-	0.73	0.59	0.48
6	0.81	0.73	0.66	0.85	0.79	0.72
7	0.68	0.39	0.23	0.80	0.80	0.79
8	0.85	0.83	0.66	0.82	0.74	0.42
9	0.70	0.49	0.40	0.75	0.72	0.57
10	0.74	0.57	0.46	0.80	0.54	0.42
Average	0.74	0.65	0.51	0.77	0.69	0.52
Std. Dev.	0.08	0.16	0.20	0.07	0.09	0.19

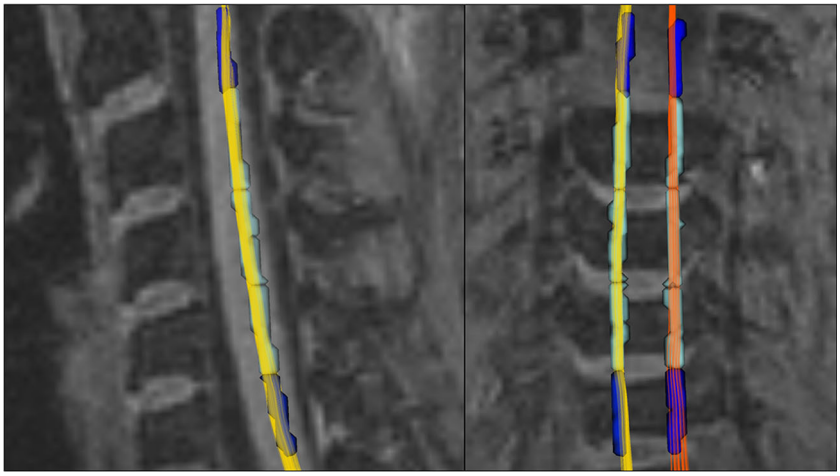

Fig. 5 Lateral (left) and sagittal (right) views of the generated fibre bundle streamlines overlaid on 3D model representations of the anatomic label maps. In this example for three skipped vertebral levels (C3–C5), the dark blue models at C2 and C6 represent the cranial and caudal seeded regions of interest (ROIs), with the light blue models (C3–C5) representing the ROI used for spatial correspondence measurements to the generated streamlines

myelotomy incision precisely between the two dorsal columns to minimize damage to the spinal cord and remove the tumour safely. This type of intramedullary procedure could benefit from tractography maps generated by DTI of the spinal cord to clearly visualize the location of the white matter tracts. For effective adoption of spinal cord tractography in computer-assisted neurosurgery, accuracy and surgeon confidence in the generated streamlines is needed. Current spinal cord resection approaches are high-risk surgeries with limited soft tissue guidance options available to the neurosurgeon. In the current study, spinal cord streamlines were most consistent with anatomical labels in an evaluation region of one vertebral level, indicating that this technique is most appropriate for geometric distortions with limited spatial extent. Further, the workflow generated in this study enabled visualization of specific white matter tract streamlines, including the ability to define specific colours for each tract, which may be useful for delineation of white matter tracts in neuro-navigation.

In general, there are several recognized challenges with clinical implementation of spinal cord imaging. These include physiological motion of the cord, the small size of the cord cross-section, and the susceptibility of the surrounding bone to introduce image artefact [11]. However, there have been recent studies supporting the preliminary use of DTI of the spinal cord in the clinical research setting [6]. For spinal cord injury conditions, there is an obvious time component to consider in ensuring patients are treated quickly and safely, potentially limiting advanced MRI sequences that require long scanning times. In the current study, the total scanning time was limited to approximately 10 min to maintain clinically viability. It is possible that better spatial correspondence may be achieved with higher signal to noise scans achieved with longer scan times or sequences available on higher-end scanners. Additionally, with the use of the template-based registration technique, detailed examination and optimization of the image acquisition sequence was not undertaken in this study. There could be opportunities to further improve the robustness of the image processing pipeline by considering alternative anatomic and diffusion-weighted imaging sequences as well as triggered acquisition with a pulse oximeter to limit motion artefacts. This study also only obtained anatomic and diffusion-weighted images from a single 3T scanner (Siemens Tim Trio); as such, translation to other scanners (1.5T or different manufacturers) could change the results. Important considerations for using 1.5T scanners for spinal cord tractography include lower signal to noise ratio (worsening results) and smaller susceptibility artefact (improving results).

Beyond image acquisition, there are limitations with respect to the image processing and data analysis conducted on only a small sample size of healthy control subjects. In this case, it is unknown how well this technique would translate to more clinically relevant datasets, which would likely include some amount of pathology. Further, due to the small and specific dataset focused on the C2–C6 region of the cervical spine, spatial correspondence was only investigated in the lateral corticospinal tracts within a focal region of interest of one to three vertebral levels. Additionally, by using a binary tract segmentation from SCT and deterministic tractography algorithm, there was likely a loss in precision that could have been avoided by considering probabilistic methods for masking (weighting partial volume) and tractography calculations [34].

Deterministic tractography algorithms were used in this investigation as part of a larger integration with the 3D Slicer platform, incorporating the SCT segmentation and registration, tractography pipeline, tract visualization analysis tools in a unified application and released open source (https://bitbucket.org/OrthopaedicBiomechanicsLab/sctwrappers/src/master/). The parameters of the tractography algorithm used were based on existing values for deterministic streamline generation reported in the literature, but no significant optimization of the parameter selection was evaluated. These parameters may also vary based on the size of the defect and the chosen size

of the ROI. Future work will include considering clinical case series, probabilistic streamline generation algorithms, and parameter optimization that produces streamlines most consistent with anatomical tract location in the spinal cord.

Conclusion

In conclusion, streamlines of the spinal cord white matter tracts of the spinal cord generated from DTI had good to fair agreement with segmentations derived from an anatomic white matter atlas, depending on the distance from the seeded vertebral level. The level of agreement between the anatomic and diffusion-based regions from this study supports further development of DTI tractography for neuro-navigation applications. This initial investigation establishes the utility of tractography-generated streamlines to define the location of individual spinal cord tracts within healthy subjects, with future work focusing on cases with pathology. This could be particularly useful in interventional applications where the pathology is isolated to a small region and the streamlines are not required to extend beyond one or more vertebral levels.

Funding This work was supported by research funding provided by FedDev Ontario, Mitacs post-doctoral fellowship support, and the Feldberg Chair for Spinal Research. Image datasets, in kind resources, and technical support were provided by Synaptive Medical Inc.

Data availability Imaging data was collected without obtaining consent for public disclosure. Therefore, it will not be made public. Specific requests for the data will be considered provided that ethics approval can be obtained for the new purpose and that a suitable transfer agreement can be established.

Compliance with ethical standards

Conflict of interest Stewart McLachlin's stipend during the research project was provided by a Mitacs fellowship with matching funds from Synaptive Medical. Jason Leung has no conflicts. Vignesh Sivan has no conflicts. Pierre-Olivier Quirion has no conflicts. Phoenix Wilkie has no conflicts. Julien Cohen-Adad has no conflicts. Cari Marisa Whyne received grant matching funds for the research reported in this article from Synaptive Medical. Michael Raymond Hardisty has no conflicts.

Ethical approval All procedures performed in studies involving human participants were in accordance with the ethical standards of the institutional and/or national research committee and with the 1964 Helsinki declaration and its later amendments or comparable ethical standards. Informed consent was obtained from all individual participants included in the study.

Consent to participate Informed consent was obtained from all individual participants included in the study (include appropriate statements).

Consent for publication Granted.

Code availability The code is available open source at https://bitbucket.org/OrthopaedicBiomechanicsLab/sctwrappers/src/master/.

References

1. Beaulieu C (2002) The basis of anisotropic water diffusion in the nervous system - a technical review. NMR Biomed 15:435–455
2. Jellison BJ, Field AS, Medow J, Lazar M, Salamat MS, Alexander AL (2004) Diffusion tensor imaging of cerebral white matter: a pictorial review of physics, fiber tract anatomy, and tumor imaging patterns. Am J Neuroradiol 25:356–369. https://doi.org/10.1038/nrn2776
3. Setzer M, Murtagh RD, Murtagh FR, Eleraky M, Jain S, Marquardt G, Seifert V, Vrionis FD (2010) Diffusion tensor imaging tractography in patients with intramedullary tumors: comparison with intraoperative findings and value for prediction of tumor resectability. J Neurosurg Spine 13:371–380. https://doi.org/10.3171/2010.3.SPINE09399
4. Chen Z, Tie Y, Olubiyi O, Zhang F, Mehrtash A, Rigolo L, Kahali P, Norton I, Pasternak O, Rathi Y, Golby AJ, O'Donnell LJ (2016) Corticospinal tract modeling for neurosurgical planning by tracking through regions of peritumoral edema and crossing fibers using two-tensor unscented Kalman filter tractography. Int J Comput Assist Radiol Surg 11:1475–1486. https://doi.org/10.1007/s11548-015-1344-5
5. Hua K, Zhang J, Wakana S, Jiang H, Li X, Reich DS, Calabresi PA, Pekar JJ, van Zijl PCM, Mori S (2008) Tract probability maps in stereotaxic spaces: analyses of white matter anatomy and tract-specific quantification. Neuroimage 39:336–347. https://doi.org/10.1016/j.neuroimage.2007.07.053
6. Martin AR, Aleksanderek I, Cohen-Adad J, Tarmohamed Z, Tetreault L, Smith N, Cadotte DW, Crawley A, Ginsberg H, Mikulis D, Fehlings MG (2015) Translating state-of-the-art spinal cord MRI techniques to clinical use: a systematic review of clinical studies utilizing DTI, MT, MWF, MRS, and fMRI. NeuroImage Clin 10:192–238. https://doi.org/10.1016/j.nicl.2015.11.019
7. Wheeler-Kingshott CA, Stroman PW, Schwab JM, Bacon M, Bosma R, Brooks J, Cadotte DW, Carlstedt T, Ciccarelli O, Cohen-Adad J, Curt A, Evangelou N, Fehlings MG, Filippi M, Kelley BJ, Kollias S, Mackay A, Porro CA, Smith S, Strittmatter SM, Summers P, Thompson AJ, Tracey I (2014) The current state-of-the-art of spinal cord imaging: applications. Neuroimage 84:1082–1093. https://doi.org/10.1016/j.neuroimage.2013.07.014
8. Egger K, Hohenhaus M, Van Velthoven V, Heil S, Urbach H (2016) Spinal diffusion tensor tractography for differentiation of intramedullary tumor-suspected lesions. Eur J Radiol 85:2275–2280. https://doi.org/10.1016/j.ejrad.2016.10.018
9. Fujiyoshi K, Konomi T, Yamada M, Hikishima K, Tsuji O, Komaki Y, Momoshima S, Toyama Y, Nakamura M, Okano H (2013) Diffusion tensor imaging and tractography of the spinal cord: From experimental studies to clinical application. Exp Neurol 242:74–82. https://doi.org/10.1016/j.expneurol.2012.07.015
10. Kelley BJ, Harel NY, Kim C-Y, Papademetris X, Coman D, Wang X, Hasan O, Kaufman A, Globinsky R, Staib LH, Cafferty WBJ, Hyder F, Strittmatter SM (2014) Diffusion tensor imaging as a predictor of locomotor function after experimental spinal cord injury and recovery. J Neurotrauma 31:1362–1373. https://doi.org/10.1089/neu.2013.3238
11. Stroman PW, Wheeler-Kingshott C, Bacon M, Schwab JM, Bosma R, Brooks J, Cadotte D, Carlstedt T, Ciccarelli O, Cohen-Adad J, Curt A, Evangelou N, Fehlings MG, Filippi M, Kelley BJ, Kollias S, Mackay A, Porro CA, Smith S, Strittmatter SM, Summers P, Tracey I (2014) The current state-of-the-art of spinal cord imaging: methods. Neuroimage 84:1070–1081. https://doi.org/10.1016/j.neuroimage.2013.04.124
12. Tykocki T, English P, Minks D, Krishnakumar A, Wynne-Jones G (2018) Predictive value of flexion and extension diffusion tensor

imaging in the early stage of cervical myelopathy. Neuroradiology 60:1181–1191. https://doi.org/10.1007/s00234-018-2097-y
13. Ellingson BM, Cohen-Adad J (2014) Diffusion-weighted imaging of the spinal cord. In: Quantitative MRI of the spinal cord. Academic Press, pp 123–145
14. Cui J-L, Li X, Chan T-Y, Mak K-C, Luk KD-K, Hu Y (2015) Quantitative assessment of column-specific degeneration in cervical spondylotic myelopathy based on diffusion tensor tractography. Eur Spine J 24:41–47. https://doi.org/10.1007/s00586-014-3522-5
15. Vargas MI, Delavelle J, Jlassi H, Rilliet B, Viallon M, Becker CD, Lövblad KO (2008) Clinical applications of diffusion tensor tractography of the spinal cord. Neuroradiology 50:25–29. https://doi.org/10.1007/s00234-007-0309-y
16. Hendrix P, Griessenauer CJ, Cohen-Adad J, Rajasekaran S, Cauley KA, Shoja MM, Pezeshk P, Shane Tubbs R (2014) Spinal diffusion tensor imaging: a comprehensive review with emphasis on spinal cord anatomy and clinical applications. Clin Anat 95:88–95. https://doi.org/10.1002/ca.22349
17. De Leener B, Lévy S, Dupont SM, Fonov VS, Stikov N, Louis Collins D, Callot V, Cohen-Adad J (2016) SCT: Spinal Cord Toolbox, an open-source software for processing spinal cord MRI data. Neuroimage 0–1. https://doi.org/10.1016/j.neuroimage.2016.10.009
18. Fonov VS, Le Troter A, Taso M, De Leener B, Lévêque G, Benhamou M, Sdika M, Benali H, Pradat P-F, Collins DL, Callot V, Cohen-Adad J (2014) Framework for integrated MRI average of the spinal cord white and gray matter: The MNI-Poly-AMU template. Neuroimage 102(Pt 2):817–827. https://doi.org/10.1016/j.neuroimage.2014.08.057
19. Lévy S, Benhamou M, Naaman C, Rainville P, Callot V, Cohen-Adad J (2015) White matter atlas of the human spinal cord with estimation of partial volume effect. Neuroimage 119:262–271. https://doi.org/10.1016/j.neuroimage.2015.06.040
20. De Leener B, Fonov VS, Collins DL, Callot V, Stikov N, Cohen-Adad J (2018) PAM50: unbiased multimodal template of the brainstem and spinal cord aligned with the ICBM152 space. Neuroimage 165:170–179. https://doi.org/10.1016/j.neuroimage.2017.10.041
21. De Leener B, Cohen-Adad J, Kadoury S (2014) Automatic 3D segmentation of spinal cord MRI using propagated deformable models. SPIE Med Imaging 9034:90343R. https://doi.org/10.1117/12.2043183
22. Fedorov A, Beichel R, Kalpathy-Cramer J, Finet J, Fillion-Robin J-C, Pujol S, Bauer C, Jennings D, Fennessy F, Sonka M, Buatti J, Aylward S, Miller JV, Pieper S, Kikinis R (2012) 3D Slicer as an image computing platform for the Quantitative Imaging Network. Magn Reson Imaging 30:1323–1341. https://doi.org/10.1016/j.mri.2012.05.001
23. Norton I, Essayed WI, Zhang F, Pujol S, Yarmarkovich A, Golby AJ, Kindlmann G, Wasserman D, Estepar RSJ, Rathi Y, Pieper S, Kikinis R, Johnson HJ, Westin CF, O'Donnell LJ (2017) SlicerDMRI: open source diffusion MRI software for brain cancer research. Cancer Res 77:e101–e103. https://doi.org/10.1158/0008-5472.CAN-17-0332
24. Andersson JLR, Skare S, Ashburner J (2003) How to correct susceptibility distortions in spin-echo echo-planar images: application to diffusion tensor imaging. Neuroimage 20:870–888. https://doi.org/10.1016/S1053-8119(03)00336-7
25. Smith SM, Jenkinson M, Woolrich MW, Beckmann CF, Behrens TEJ, Johansen-Berg H, Bannister PR, De Luca M, Drobnjak I, Flitney DE, Niazy RK, Saunders J, Vickers J, Zhang Y, De Stefano N, Brady JM, Matthews PM (2004) Advances in functional and structural MR image analysis and implementation as FSL. Neuroimage 23:S208–S219. https://doi.org/10.1016/J.NEUROIMAGE.2004.07.051
26. Alexander DC, Pierpaoli C, Basser PJ, Gee JC (2001) Spatial transformations of diffusion tensor magnetic resonance images. IEEE Trans Med Imaging 20:1131–1139. https://doi.org/10.1109/42.963816
27. Dupont SM, De Leener B, Taso M, Le Troter A, Nadeau S, Stikov N, Callot V, Cohen-Adad J (2017) Fully-integrated framework for the segmentation and registration of the spinal cord white and gray matter. Neuroimage 150:358–372. https://doi.org/10.1016/j.neuroimage.2016.09.026
28. Maki S, Koda M, Saito J, Takahashi S, Inada T, Kamiya K, Ota M, Iijima Y, Masuda Y, Matsumoto K, Kojima M, Takahashi K, Obata T, Masashi Yamazaki TF (2016) Tract-specific diffusion tensor imaging reveals laterality of neurological symptoms in patients with cervical compression myelopathy. World Neurosurg 96:184–190. https://doi.org/10.1016/j.wneu.2016.08.129
29. Lundell H, Barthelemy D, Biering-Sørensen F, Cohen-Adad J, Nielsen JB, Dyrby TB (2013) Fast diffusion tensor imaging and tractography of the whole cervical spinal cord using point spread function corrected echo planar imaging. Magn Reson Med 69:144–149. https://doi.org/10.1002/mrm.24235
30. Bosma R, Stroman PW (2012) Diffusion tensor imaging in the human spinal cord: development, limitations, and clinical applications. Crit Rev Biomed Eng 40:1–20. https://doi.org/10.1615/CritRevBiomedEng.v40.i1.10
31. Ducreux D, Fillard P, Facon D, Ozanne A, Lepeintre JF, Renoux J, Tadi M, Lasjaunias P (2007) Diffusion tensor magnetic resonance imaging and fiber tracking in spinal cord lesions: current and future indications. Neuroimaging Clin N Am 17:137–147. https://doi.org/10.1016/j.nic.2006.11.005
32. Dauleac C, Frindel C, Mertens P, Jacquesson T, Cotton F (2020) Overcoming challenges of the human spinal cord tractography for routine clinical use: a review. Neuroradiology 62:1079–1094
33. Wang K, Chen Z, Zhang F, Song Q, Hou C, Tang Y, Wang J, Chen S, Bian Y, Hao Q, Shen H (2016) Evaluation of DTI parameter ratios and diffusion tensor tractography grading in the diagnosis and prognosis prediction of cervical spondylotic myelopathy
34. Tournier JD, Calamante F, Connelly A (2012) MRtrix: diffusion tractography in crossing fiber regions. Int J Imaging Syst Technol 22:53–66. https://doi.org/10.1002/ima.22005